



Project	GUTTA
Work Package number	3
Work Package title	Strategic potential for a greener and more integrated CB maritime mobility
Deliverable number	3.2.3.
Deliverable title	Report on the literature survey of optimization algorithms
Deliverable Responsible Partner	CMCC
Deliverable Lead authors	Gianandrea Mannarini (CMCC)
Deliverable Contributors	
Deliverable due date	2019-12-31
Deliverable latest review date	2020-02-11

Table of Contents

Table of Contents	1
Executive Summary	1
1. Introduction	1
2. Vessel speed modelling.....	1
a. Wind.....	2
b. Waves.....	4
2.3 Currents	7
2.4 CO ₂ emissions	7
3 Path planning.....	7
3.1 Shortest path algorithms	8
3.2 Constrained optimization.....	8
Conclusions	10
References	10

Executive Summary

This report includes information about the algorithms to be used by the eco-route planning tool corresponding to SO.1 of GUTTA project.

The planning tool will be based on the VISIR ship routing model. At the heart of VISIR are two crucial model components: the vessel seakeeping/emission model, and the routine for optimization of the marine path. Both components are addressed in this report.

1. Introduction

Possible updates to the vessel seakeeping and propulsion model of VISIR-1 are described in Sect.2 and Sect.3, while the various path optimization strategies are presented in Sect.4.

2. Vessel speed modelling

According to the ISO 15016:2015 standard (s. Bibliography), the environmental fields most impacting speed and power performance of vessels are: wind, sea state (i.e., surface gravity waves), water temperature and density (for their effect on viscosity), and sea currents.

In GUTTA D.3.1.4. a catalogue of the operational availability of forecast maps of these fields is provided.

GUTTA will deliver, through deliverable D. 4.1.1 (due at project month M20), a parametrization of CO2 emissions for a specific type of RoPax vessel operating on IT-HR cross border routes, in terms of a few environmental state variables. In the meanwhile, a vessel-generic model is needed to set up and test the new VISIR-2 code.

For the modelling of the effect of wind and waves on ferries, we refer to the ITTC 7.5-04 -01-01.2 document (ITTC, 2014). It reports an assessment of actual ship performance by analysis of speed trial data. To this end, it includes a method for computing the added resistances due to waves and wind. The equations for the added resistances reported thereto (Sect.3.1-2) can be used in VISIR-2 for estimating the speed through water (STW). It is then combined as in Mannarini & Carelli (2019) with the sea currents for obtaining the speed over ground (SOG; Sect.3.3). We note that most of the information from the ITTC document is also reported in the ISO-15016:2015 standard (ISO, 2015).

The effect of water temperature and water density can be considered of second order with respect to wind, waves, and currents. Thus, water temperature and water density will be neglected in this treatment and, correspondingly, in the first version of VISIR-2.

a. Wind

Wind affects vessel performance both directly (through the added aerodynamic resistance of the superstructure) and indirectly via wind generated waves (cf. Sect.3.2) that lead to an additional resistance.

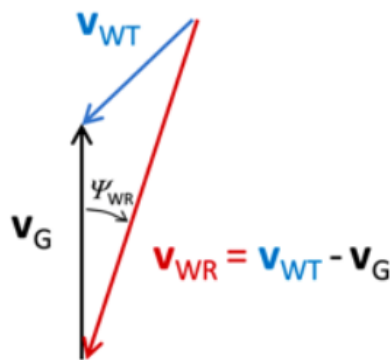


Figure 1 Geometry of the wind-ship interaction: V_{WT} is the true wind speed, V_G is the ship velocity (not distinguishing between SOG and STW) and V_{WR} is the relative wind speed.

In (ITTC, 2014) Eq. 5 allows to compute the resistance increase due to wind, R_{AA} .

$$R_{AA} = \frac{1}{2} \rho_A V_{WR}^2 C_X (\psi_{WR}) A_{XV} \quad (5)$$

A few remarks may be helpful:

- Eq.5 of (ITTC, 2014) corresponds to Eq.C.1 of (ISO, 2015):
 - ISO quantifies the resistance *increase* due to wind, thus it vanishes for zero wind;
 - ITTC quantifies the resistance increase due to *relative* wind, thus it does not vanish for zero wind ($V_{WT}=0$ does not imply $V_{WR}=0$; cf. Figure 1)
- C_X of Eq.5 does not only includes ship frontal but also ship lateral section, as well as other ship parameters as per Fig.C.2 of ITTC (2014), also reported In Figure 2 and Table 1 of this report.
- The note in (ITTC,2014) that $C_X=-C_A$ probably refers to the fact that the plots in App.C, Fig.C-1 should be inverted.
- Following on the previous bullet, a reasonable initial approximation is: $C_X = 1 - \psi/\pi$

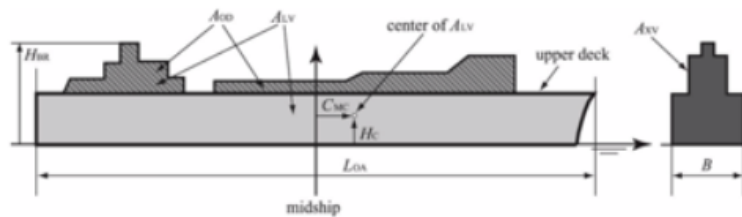


Figure Input parameters for regression formula by Fujiwara et al., 2006, as reported in Fig.C.4 of ISO (2015) which is clearer than Fig.C.2 of ITTC (2014).

Table 1 Ship geometry parameters needed for application of Fujiwara's method, distinguishing between the original paper by Fujiwara (2006), the ITTC (2014), and the ISO (2015) documents.

			Name	units
Fujiwara 2006	ITTC, 2014	ISO, 2015		
B	B	B	breadth	m
A _{OD}	A _{OD}	A _{OD}	lateral projected area of superstructure on the deck	m ²
C	C _{MC}	C _{MC}	horizontal distance from amidships section to center of lateral projected area	m
H _C	H _C	H _C	height from calm water surface to center of lateral projected area	m
H _{BR}	H _{BR}	H _{BR}	height of top of superstructure	m

L_{OA}	L_{OA}	L_{OA}	Length overall	m
A_F	A_{XV}	A_{XV}	frontal projected area	m^2
A_L	A_{YV}	A_{LV}	lateral projected area	m^2

b. Waves

Waves are another important environmental field acting on the vessel. The so called “total sea” consists of both wind waves and swell, see Figure 2 Relation between wind-waves and swell. Source: ECMWF, ocean wave forecasting.

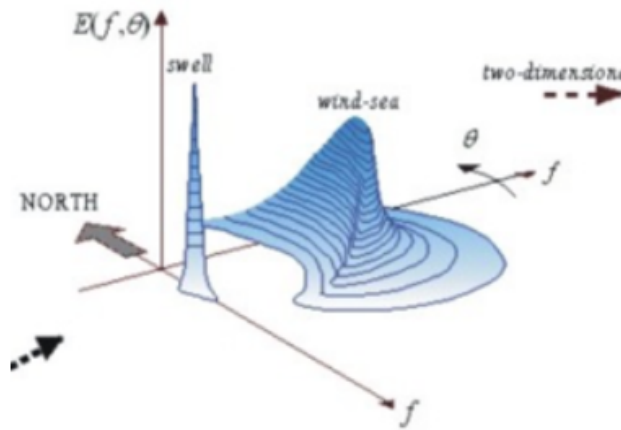


Figure 2 Relation between wind-waves and swell. Source: ECMWF, ocean wave forecasting.

The following treatment refers to irregular waves, as in the typical spectrum of wind-waves, but is general enough to be used for describing the swell component too. However, swell is generally negligible in the Adriatic (compared e.g. to Atlantic-IBI region, cf. Fig.3).

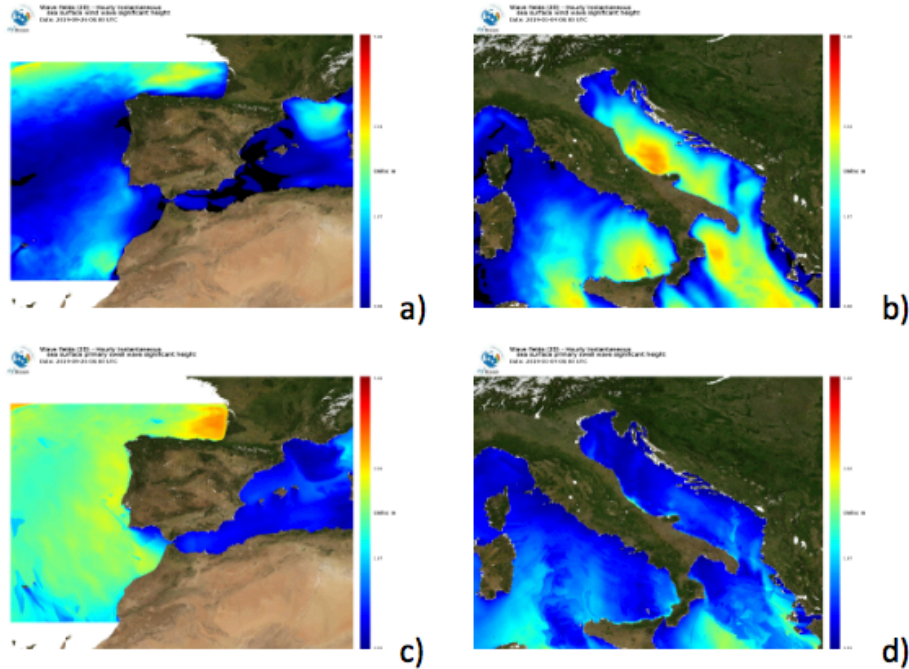


Figure 3 Exemplary wind-wave (upper panels) and swell (lower panels) situation in the Ireland-Biscay-Iberian region (a,c) and in the Adriatic Sea (b,d) from model outputs provided through the European service CMEMS.

We refer in this subsection to the ITTC (2014) that presents a more concise treatment than ISO (2015). In Eq.6, the general relation between the wave added resistance in regular waves $R_{wave}(\omega, \alpha, V_s)$ and the resistance R_{AW} in irregular waves is stated:

$$R_{AW} = 2 \int_0^{2\pi} \int_0^{\infty} \frac{R_{wave}(\omega, \alpha; V_s)}{\zeta_A^2} E(\omega, \alpha) d\omega d\alpha \quad (6)$$

The directional spectrum $E(\omega, \alpha)$ factorizes into a frequency spectrum $S(\omega)$ and an angular distribution function $G(\alpha)$. For ocean waves, $S(\omega)$ is a modified Pierson-Moskowitz spectrum. In the simplest case, $G(\alpha)$ is a cosine function of wave-ship relative angle α , cf. Figure 4.

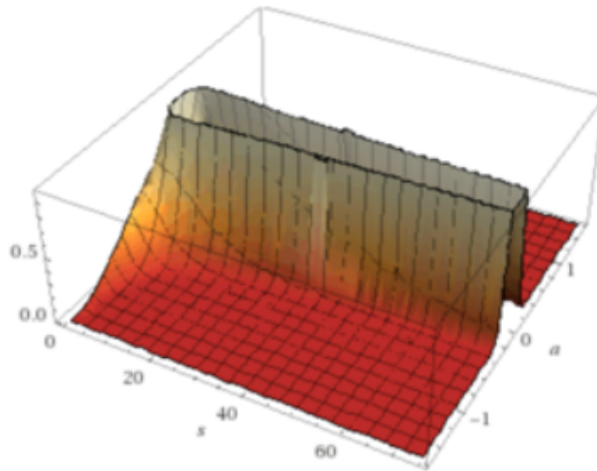


Figure 4 The $G(a,s)$ function where a is the wave-ship relative angle and s is the directional spreading parameter. Plot realized from Eq.12 of ITTC (2014) via WolframAlpha.

The resistance in regular waves $R_{wave}(\omega, \alpha, Vs)$ requires a specific treatment.

ITTC (2014) presents four levels of accuracy, of which only the first three are briefly reported here (the fourth one is based on towing tank tests and includes just a reference to the test set-up and procedure):

- Direct correction method STAwave-1
This applies to short head waves. In this case, the encounter frequency of the waves is high. Thus, the effect of wave induced motions can be neglected and the added resistance is dominated by the wave reflection. The resulting formula (R_{AWL} in D-1) is quite simple and its application is restricted to waves from the bow sector.
- Empirical transfer function STAwave-2
Based on extensive seakeeping model test results for large population of ships, this method allows to cover both the mean resistance increase due to wave reflection R_{AWR} (D-2) and the motion induced resistance R_{AWM} (D-3).
- Theoretical computation
Based on Maruo's theory for estimating the resistance due to ship motion (R_{AWM}), the treatment includes a correction term primarily valid for short waves (R_{AWR}).

2.3 Currents

Vessel STW (F) and sea surface currents (w) are linearly superposed as in Mannarini & Carelli (2019) for computing SOG,

$$S_g = w_{\parallel} + \sqrt{F^2 - w_{\perp}^2}.$$

where F is the STW (depending on waves and wind) and w is the sea current field.

2.4 CO₂ emissions

The mass of emitted CO₂ depends on vessel engine, fuel type, and duration of the emissions.

In particular, vessel engine power P , route duration T , fuel specific consumption s , and the conversion factor C_F from fuel consumption to mass of CO₂ emitted, are used to compute M_{CO_2} as:

$$M_{CO_2} = P \cdot T \cdot s \cdot C_F$$

More information on this can be found e.g. in IMO (2009).

3 Path planning

Per GUTTA's AF, "VISIR shortest path algorithm will be updated for computing routes of given ETA and minimum CO₂ emissions" (Activity 4.1).

ETA or "Estimated Time of Arrival" refers to the planned time at which the vessel calls at the arrival port. The assignment of ETA corresponds to the stipulated schedule that ferries must observe in order to comply with both passengers' rights and harbour logistics.

Fulfilling an ETA is equivalent to say that the duration of the voyage is constant and does not vary with the actual sea conditions experienced by the vessel.

Computing routes of given ETA and minimum CO₂ emissions represents a significant conceptual change with respect to the VISIR versions ("VISIR-1") released so far. In fact, VISIR-1 aimed to compute least-time routes, which is a kind of *single-objective* optimization, while the new developments ("VISIR-2") call for a *constrained-optimization*: minimum emissions (cf. Sect.3.4) and given ETA.

In the following subsections, the key ingredients for solving the constrained-optimization problem are reviewed: the shortest path algorithms, used for computing path optimizing single objectives; the sailing options, corresponding to the optimization options offered to the end-users of the new VISIR system; the technique for constrained optimization.

3.1 Shortest path algorithms

The VISIR-2 code uses the python library networkx¹. Thus, it can employ the various shortest path algorithms of the library. The most promising ones for the purposes of the GUTTA project are:

- Dijkstra: Returns the shortest path from source to target in a weighted graph G in a time $O(A+N \log N)$, with a N number of nodes and A number of arcs;
- A*: even faster than Dijkstra in presence of a proper heuristic;
- Bellman Ford: It is slower than Dijkstra but can handle negative edge weights;
- Yen's algorithm: A generator that produces lists of simple paths, in order from shortest to longest.

3.2 Constrained optimization

First of all, important to classify the exact nature and scope of the problem. This can be done by following keywords that progressively define it:

- Pareto optimization, cf. Figure 5
- bi-criterion problems/ bicriteria shortest path problem (SPP)
- resource constrained optimization (RCSPP)
- shortest path problem with time window (SPPTW)
- vehicle routing problem with time windows (VRPTW)

The SPP requires finding an (s,t) -path of minimum length for any given nodes s and t . The RCSPP problem inputs an additional budget b , and requires finding a minimum length (s,t) -path with total cost less than b . The two problems, though similar, have very different runtime complexity: SPP queries admit polynomial-time algorithms (in particular, the famous Dijkstra's algorithm), while RCSPP computation is known to be NP-Hard. That said, a standard dynamic program computes RCSPP in pseudo-polynomial time for discrete costs [Vera et al, 2017].

Exact methods appearing in the literature that apply to the WCSPP can be divided into those based on k th-shortest paths [Choudhury, 2015], node-labeling methods derived from dynamic programming equations, and Lagrangean relaxation [Jüttner, 2005], although some work combines these approaches.

¹ <https://networkx.github.io/documentation/stable/index.html>

In addition to exact algorithms, approximation algorithms have been developed, based on cost scaling [Dumitrescu and Boland, 2003].

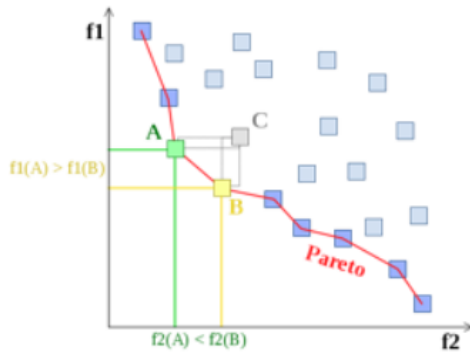


Figure 5 Example of a Pareto frontier. The boxed points represent feasible choices, and smaller values are preferred to larger ones. Point C is not on the Pareto frontier because it is dominated by both point A and point B. Points A and B are not strictly dominated (source: Wikipedia).

Conclusions

This report contributes to the development of the VISIR-2 model with respect to the vessel seakeeping and emission parametrization and the computation of constrained optimal routes. The research work on these topics in GUTTA project is still ongoing and this report just provides an initial reference to further refine the literature investigation in view of the actual needs of the project.

References

Fujiwara, T., Ueno, M. and Ikeda, Y., 2006, January. Cruising performance of a large passenger ship in heavy sea. In The Sixteenth International Offshore and Polar Engineering Conference. International Society of Offshore and Polar Engineers.

Grin, R.: On the Prediction of Wave-added Resistance with Empirical Methods, Journal of Ship Production and Design, 31, 181– 191, 2015.

IMO (2009): MEPC.1/Circ.684 Guidelines for voluntary use of the ship Energy Efficiency Operational Indicator (EEOI), Tech. rep., International Maritime Organization, London, UK.

ISO (2015): IMO MEPC 68/INF.14 (Annex) "ISO 15016:2015". Technical report, International Maritime Organization, London, UK, 2015.

ITTC (2014): Recommended Procedures and Guidelines 7.5-04-01-01.2

G. Mannarini and L. Carelli. VISIR-1.b: ocean surface gravity waves and currents for energy-efficient navigation. Geoscientific Model Development, 12(8):3449–3480, 2019.

<https://www.geosci-model-dev.net/12/3449/2019/gmd-12-3449-2019.html>

G. Mannarini, N. Pinardi, G. Coppini, P. Oddo, and A. Iafrazi. VISIR-I: small vessels – least-time nautical routes using wave forecasts. Geoscientific Model Development, 9(4):1597–1625, 2016.

<https://www.geosci-model-dev.net/9/1597/2016/>